ELSEVIER

Chemical Engineering Journal 132 (2007) 233–239

Chemical Engineering Journal

www.elsevier.com/locate/cej

Desorption activation energy of dibenzothiophene on the activated carbons modified by different metal salt solutions

Moxin Yu, Zhong Li *, Qibin Xia, Hongxia Xi, Shuwen Wang

School of Chemical and Energy Engineering, South China University of Technology, The Key Laboratory of Enhanced Heat Transfer and Energy Conversation Ministry of Education, Guangzhou 510640, PR China

Received 28 July 2006; received in revised form 22 December 2006; accepted 5 January 2007

Abstract

This work mainly involved the investigation of the effects of different metal ions loaded on activated carbons on activation energy for desorption of dibenzothiophene (DBT). Five kinds of transition metal ions were separately loaded on the activated carbons by impregnation method. Temperature-programmed desorption (TPD) experiments were conducted to measure the TPD curves of DBT on these modified activated carbons, and the desorption activation energy, E_d, of DBT on the activated carbon surfaces were estimated. The variation of E_d of DBT on the activated carbons was discussed with the help of hard and soft acid and base (HSAB) principle. Results indicated that each of TPD spectrum for DBT desorption on the activated carbons loaded separately with Ag^+, Ni^{2+}, Cu^{2+} and Zn^{2+} showed two distinct peaks, respectively corresponding to interaction of DBT with the activated carbon surface and with the metal ions, which indicated producing new adsorption sites. The desorption activation energy of DBT on the activated carbons Ag(I)/AC, Zn(II)/AC, Ni(II)/AC, Cu(II)/AC, AC and Fe(III)/AC were 92.96, 88.64, 74.91, 69.32, 54.65 and 47.39 kJ/mol, respectively. In comparison with the original activated carbon, the loading of Ag^+ enhanced the interaction between DBT and Ag(I)/AC surfaces because Ag^+ was soft acid and DBT was soft base, and the loading of Fe^{3+} weakened the interaction between DBT and Fe(III)/AC surfaces because Fe^{3+} was hard acid, while DBT was soft base. The loading of the borderline acid ion Zn^{2+}, Ni^{2+} or Cu^{2+} on the surfaces of the activated carbon could weaken the local hard acids of the surfaces so that adsorption of DBT was enhanced to some extent.

Keywords: Temperature-programmed desorption; Dibenzothiophene; Activated carbon; Desorption activation energy; HSAB principle

1. Introduction

Deep desulfurization of transportation fuels is receiving increasing attention in the research community worldwide due to increasingly stringent regulations and fuel specifications in many countries since combustion of the fuels containing sulfur produces SO_2. The US EPA mandates a reduction in gasoline and diesel sulfur levels to 30 and 15 ppmw, respectively, from the current levels of 300–500 ppmw, to be implemented by 2006. In 2010, the maximum S-content will be limited to 10 ppmw, European legislation also restricts the sulfur level to less than 50 ppmw for both fuels by 2005 and 10 ppmw by 2008 [1]. For both environment protection and market competition, Chinese government sets the objectives for the sulfur level to less than 10 ppmw by 2010 from the current levels of less than 800 ppmw for gasoline and 2000 ppmw for diesel except 150 ppmw in several big cities like Beijing and Shanghai. Hence a considerable effort is being made to remove the organosulfur molecules from the fuel to obtain sulfur free or ultra-low-sulfur fuel.

Although number of organic sulfur compounds present in the fuels, aromatic sulfur compounds such as thiophene (T), benzothiophene (BT), dibenzothiophene (DBT) or methyl substituted dibenzothiophene are of prime concern. Conventional hydrotreating process can remove the most of the organic sulfur compounds present in the fuels. However, it also results in a significant reduction of octane number due to the saturation of olefins. The refractory benzothiophenic sulfur compounds in diesel are very difficult to desulfurize to achieve a total sulfur level of less than 15 ppmw using conventional hydrotreating processes [1]. So, alternative technologies are of particular interest to obtain sulfur free fuels. One of the new approaches for desulfurization is by selective adsorption of the sulfur compounds on adsorbents. Adsorption technology might be the most economical way for the removal of the sulfur compounds since it does not need treating the whole fuel under high pressure and temperature. It is well known that the adsorbent is the core of

* Corresponding author. Fax: +86 20 87113735.
E-mail address: cezhli@scut.edu.cn (Z. Li).

1385-8947/$ – see front matter © 2007 Elsevier B.V. All rights reserved.
doi:10.1016/j.cej.2007.01.003

adsorption technology. Recent years, a series of desulfurization adsorption adsorbents have been explored. Song et al. explored a process which was called selective adsorption for removing sulfur (PSU-SARS) over various materials under ambient conditions for fuel cell and refinery applications [2–4]. Various adsorbents including metals, metal halides, metal oxides, metal sulfides, and modified zeolites were synthesized and evaluated [5–7]. Among several types of adsorbents explored, Ni-based adsorbents exhibited better performance for removing sulfur compounds [7]. Yang and co-workers have developed a variety of π-complexation-based sorbents obtained by ion exchanging zeolites with different metal cations. Among them, Cu(I)/Y-zeolite had the best adsorption performance for thiophenic sulfur [8–11]. Activated carbons with large surface areas, rich pore structures and abundant surface groups were also used to desulfurization. Activated carbon, zeolite 5A and zeolite 13X were used for naphtha desulfurization [12,13]. Zeolite 13X showed some capacity for sulfur at low concentration ranges. At higher ranges the capacity of activated carbon was three times greater than that of 13X zeolite. Zeolite 5A was unfavorable for sulfur sorption from naphtha. More recently, Kim et al. reported that activated carbon was used as adsorbent for desulfurization of a model diesel [14], and they found that the activated carbon showed higher adsorptive capacity and selectivity for sulfur compounds, especially for the sulfur compounds with methyl substituents, such as 4,6-methyldibenzothiophene. Furthermore, Hernandez-Maldonado et al. reported that the use of activated carbon as adsorbent in a guard bed can improve the adsorptive performance of Cu(I)–Y zeolites [15]. Although the activated carbon has proven to adsorb sulfur compounds, it cannot be industrially used because its adsorption capacity was not high enough for commercial desulfurization. Therefore, modification of activated carbon surfaces is necessary to its sulfur adsorption capacity.

The purpose of this work is to investigate the effects of loading five different metal ions Ag^+, Cu^{2+}, Ni^{2+}, Zn^{2+} or Fe^{3+} onto the activated carbons on the activation energy for DBT desorption from the carbon surfaces by means of temperature-programmed desorption technique (TPD) and hard and soft acids and bases (HSAB) principle.

2. TPD model and theory

TPD technique is a technique of surface analysis [16–20]. It is usually used to estimate binding energy between an adsorbate and an adsorbent, and activation energy of desorption, which can be used to value the adsorbents. The activation energy of desorption, E_d, can be found out by following equation:

$$\ln\left(\frac{RT_p^2}{\beta_H}\right) = \frac{E_d}{R}\left(\frac{1}{T_p}\right) + \ln\left(\frac{E_d}{k_0}\right) \quad (1)$$

where R is the gas constant; T_p the peak temperature of the TPD (K); β_H heating rate (K/min); E_d activation energy of desorption (kJ/mol); k_0 is the coefficient of desorption rate. If a series of TPD experiments are conducted at different heating rates, corresponding TPD curves and values T_p could be obtained. After that, a plot of $\ln(RT_p^2/\beta_H)$ versus $1/T_p$ will yield a line with slope E_d/R. As a result, from the slope of the line, E_d can be found out, and then k_0 can be also obtained from the intercept of the line.

3. Experiments

3.1. Materials and instruments

The adsorbate, dibenzothiophene (98%), was purchased from Acros Organics, NJ, USA. The activated carbon (40–60 mesh) based on coconut shell was supplied by Zhaoyang Senyuan Activated Carbon Company, China. $AgNO_3$, $Cu(NO_3)_2$, $Ni(NO_3)_2$, $Zn(NO_3)_2$, $Fe(NO_3)_3$ and methanol, were all analytical reagents.

The TPD process was performed in a fixed-bed mini reaction furnace (LW4, Jiangsu, China). The diameter of the differential fixed bed was 0.2 cm and its length was 0.5 cm. Desorption temperature was controlled by a temperature-programmed controller (Al-708, Xiamen, China). The desorbed products were continuously determined by a gas chromatograph with a flame ionization detector (GC-950, Shanghai, China).

3.2. Experimental methods

3.2.1. Preparation of TPD samples

The activated carbons were impregnated into 100 ml 0.1 M $AgNO_3$, $Cu(NO_3)_2$, $Ni(NO_3)_2$, $Zn(NO_3)_2$, or $Fe(NO_3)_3$ aqueous solution respectively at room temperature for 12 h. Subsequently the resulting mixtures were separately filtered and dried at 393 K for 5 h. Six sorbents including the original activated carbon (AC), Ag(I)/AC, Cu(II)/AC, Ni(II)/AC, Zn(II)/AC and Fe(III)/AC were separately used in the TPD experiments. The TPD samples were prepared by impregnating the above adsorbents respectively into 5 ml of 0.02 M solution of DBT in methanol for 30 min. Subsequently the samples were filtered and kept at room temperature for 24 h under a continuous flow of air to remove the residual methanol.

3.2.2. TPD experiments

Fig. 1 shows the flow chart of TPD equipment. The TPD experiments were conducted respectively at different heating rates from 5 to 10 K/min. In each experiment, the sample that had adsorbed DBT was packed in a stainless reaction tube whose inner diameter and length were respectively 0.2 and 0.5 cm. Sub-

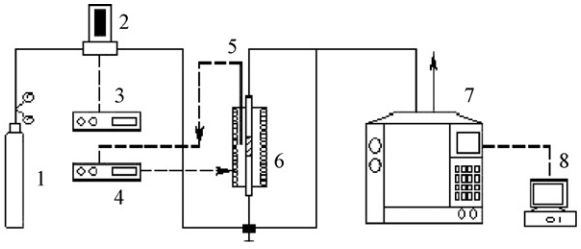

Fig. 1. Schematic flow diagram of temperature-programmed desorption (TPD): (1) N_2; (2) mass flow meter; (3) mass flow rate controller; (4) temperature controller; (5) thermal couple; (6) mini reaction furnace; (7) GC (FID); (8) GC work station.

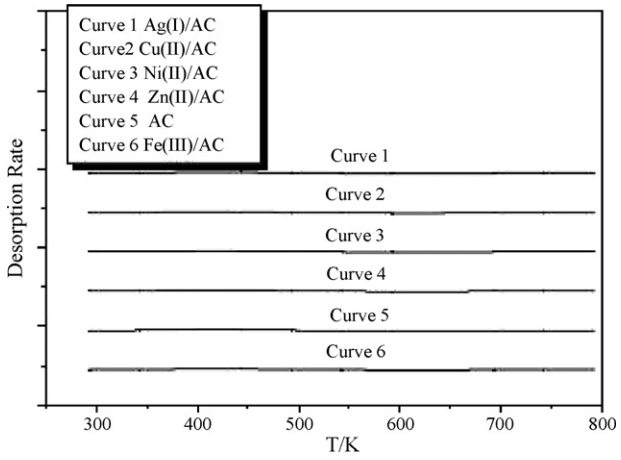

Fig. 2. TPD spectrums of the six different activated carbons, experimental condition: β_H = 5 K/min (flowrate: 50 ml/min).

sequently the stainless tube was placed in a reaction furnace and then heated in the high-purity N_2 flow at a constant rate 50 ml/min. The desorbed DBT was measured by GC at the outlet of the column, and effluent curves were recorded, which were called the TPD curves.

4. Results and discussion

4.1. Spectrum analysis

Fig. 2 shows TPD spectrums of the six different activated carbons, Ag(I)/AC, Cu(II)/AC, Ni(II)/AC, Zn(II)/AC, original activated carbon and Fe(III)/AC at the heating rate of 5 K/min. It would be noted that there were no obvious peaks in the TPD spectra obtained as none of the activated carbons was associated with any adsorbate.

Fig. 3 shows TPD spectrums of DBT desorption on the original activated carbon which adsorbed DBT at different heating rates from 5 to 10 K/min. It was seen that there were two peaks in a TPD spectrum. Each peak represented a different kinetic process: the first one was the desorption peak of residual solvent, and the second one was that of DBT adsorbed on the

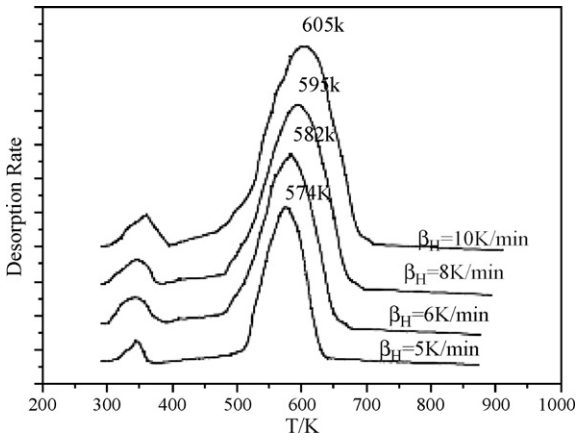

Fig. 3. Effect of β_H on TPD spectrum for the desorption of DBT on the original activated carbon (flowrate: 50 ml/min).

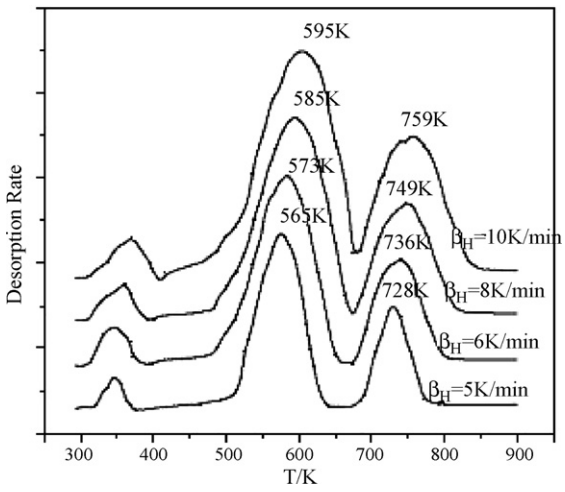

Fig. 4. Effect of β_H on TPD spectrum for the desorption of DBT on Ag(I)/AC (flowrate: 50 ml/min).

activated carbon. Figs. 4–7 depict TPD spectrum of DBT desorption on the activated carbons Ag(I)/AC, Cu(II)/AC, Ni(II)/AC and Zn(II)/AC which adsorbed DBT. Different from Fig. 3, there were obviously three peaks in a TPD spectrum. The first

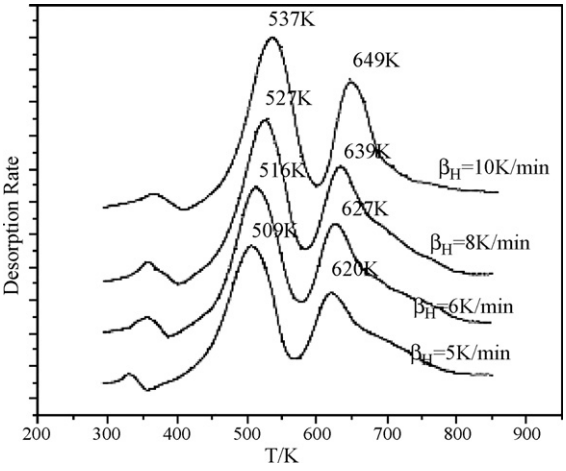

Fig. 5. Effect of β_H on TPD spectrum for the desorption of DBT on Cu(II)/AC (flowrate: 50 ml/min).

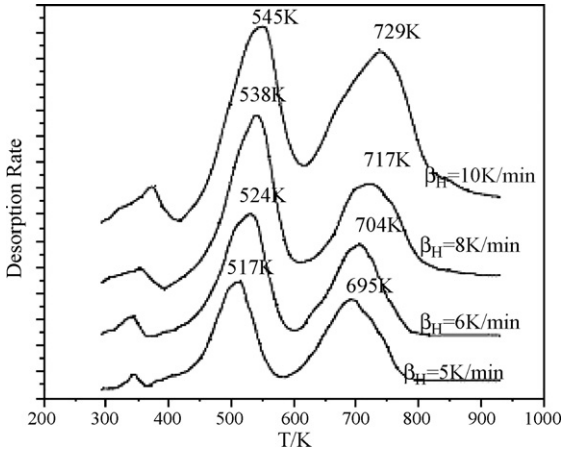

Fig. 6. Effect of β_H on TPD spectrum for the desorption of DBT on Ni(II)/AC (flowrate: 50 ml/min).

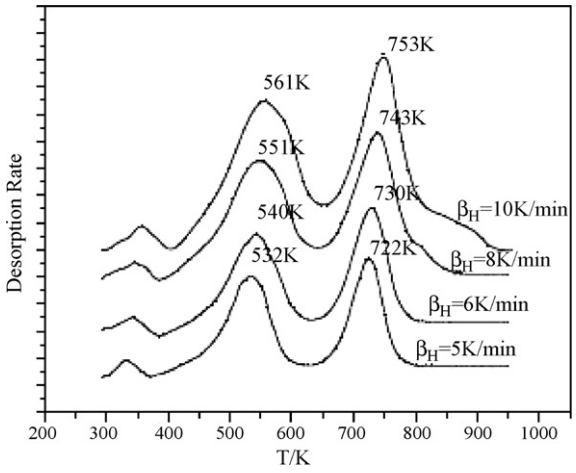

Fig. 7. Effect of β_H on TPD spectrum for the desorption of DBT on Zn(II)/AC (flowrate: 50 ml/min).

one was the desorption peak of the residual solvent, and however, the other two peaks appearing for the DBT desorption showed that there were two kinds of adsorption active sites on the surfaces of the modified activated carbons, of which the first one came from the desorption of DBT reacted to the surface of the activated carbon, and the second one possibly came from the desorption of DBT reacted to the Ag^+, Cu^{2+}, Ni^{2+} or Zn^{2+} metal ion of the surfaces of the activated carbons.

Noticeably, Fig. 8 shows the TPD spectrum of the DBT desorption on Fe(III)/AC. It could be seen that only one peak can be observed, which implied that the loading of Fe^{3+} onto the surface of activated carbon did not make more adsorption active sites appear. At the same time, it could be seen that the desorption peak temperatures T_p of DBT on Fe(III)/AC were lower than that on the original activated carbon as shown in Fig. 3, which implied that the adsorption of DBT on Fe(III)/AC would be possibly weakened in comparison with that on the original activated carbon.

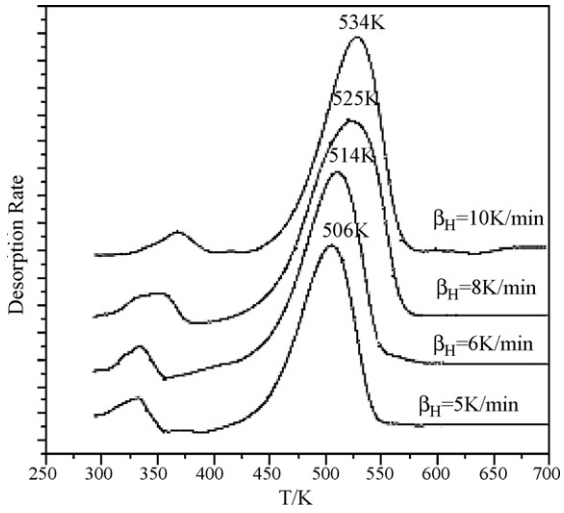

Fig. 8. Effect of β_H on TPD spectrum for the desorption of DBT on Fe(III)/AC (flowrate: 50 ml/min).

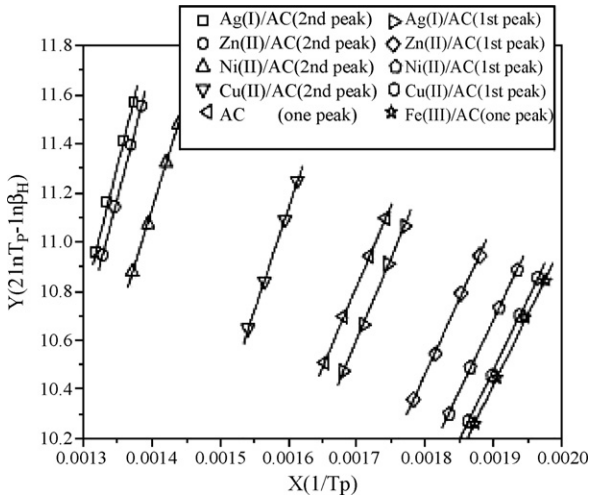

Fig. 9. Linear dependence between $\ln(RT_p^2/\beta_H)$ and $1/T_p$ for TPD of DBT on various activated carbons.

4.2. Estimation of desorption activation energy

Once a series of the TPD spectrums of DBT desorption on the activated carbon at different heating rates were available, the desorption activation energy of DBT can be estimated using Eq. (1). The linear dependence on $1/T_p$ of $\ln(RT_p^2/\beta_H)$ for the TPD of DBT on the activated carbons were shown in Fig. 9. From the slope of these lines, activation energy E_d can be found out, and then k_0 can be also obtained from the intercept of these lines. The desorption activation energy of DBT on the activated carbons studied in this work are listed in Table 1. It was noticeable that the TPD spectrums of DBT desorption on AC and Fe(III)/AC were different from those on Ag(I)/AC, Cu(II)/AC, Ni(II)/AC and Zn(II)/AC. The former only had one peak representing for the DBT desorption as shown in Figs. 3 and 8, while the later had two peaks representing for the DBT desorption as shown in Figs. 4–7. If a TPD spectrum showed two peaks representing for the DBT desorption, it possibly implied the desorption of DBT came from two kinds of adsorptive sites at least. Therefore, the activation energy of the DBT desorption on the activated carbon surfaces can be estimated according to the first peak temperature of each TPD curve, and then that on the activated carbon surfaces occupied by Ag^+, Cu^{2+}, Ni^{2+} or Zn^{2+} metal ion can be found out on the basis of the second peak temperature of each TPD curve. Table 1 lists the desorption activation energy, E_d, of DBT on the various activated carbons. It showed that the E_d of DBT estimated by using the second peak temperature of the TPD curve was higher than that by using the first peak temperature of the TPD curve, and it was also higher than that on the original activated carbon, which suggested that the loading of Ag^+, Cu^{2+}, Ni^{2+} or Zn^{2+} metal ion onto the surfaces of the activated carbons enhanced the interaction between DBT and the surfaces.

On the other hand, it was found that the E_d of DBT on Fe(III)/AC was lower than that on the original activated carbon, which meant the loading of Fe^{3+} metal ion onto the surfaces of the activated carbon weakened the adsorption of DBT on the surfaces. The activation energy for the desorption, E_d, of DBT on the activated carbons followed the

Table 1
Activation energy for desorption of DBT on various activated carbons

Activated carbons	Peaks	T_p (K) corresponding to peak of TPD curves at different heating rate β_H (K/min)				E_d (kJ/mol)
		5	6	8	10	
Ag(I)/AC	First peak	565	573	585	595	53.47
	Second peak	728	736	749	759	92.96
Cu(II)/AC	First peak	509	516	527	537	47.88
	Second peak	620	627	639	649	69.32
Ni(II)/AC	First peak	517	524	536	545	48.86
	Second peak	695	704	717	729	74.91
Zn(II)/AC	First peak	532	540	551	561	50.92
	Second peak	722	730	743	753	88.64
AC	One peak	574	582	595	605	54.65
Fe(III)/AC	One peak	506	514	525	534	47.39

order: Ag(I)/AC > Zn(II)/AC > Ni(II)/AC > Cu(II)/AC > AC > Fe(III)/AC.

Generally speaking, the higher the desorption activation energy was, the more difficult the desorption of the adsorbate from an adsorbent was. In other words, the higher the desorption activation energy was, the stronger the adsorption of the adsorbate on the surfaces of the adsorbent was. The above results indicated that the loading of transition metal ions Ag^+, Cu^{2+}, Ni^{2+} and Zn^{2+}could enhanced the interaction between DBT and activated carbon, while the loading of metal ion Fe^{3+} could weaken the interaction between DBT and activated carbon.

4.3. Effect of local hardness of activated carbon surface on activation energy of DBT desorption

Generally speaking, adsorption property of an adsorbent not only was determined by its porous microtexture but was also strongly influenced by the chemical property of its surface [21]. It can be seen from Table 1 that the loading of Ag^+, Cu^{2+}, Ni^{2+}, Zn^{2+} or Fe^{3+} ion on the surfaces of the activated carbons resulted in the variation of activation energy of the DBT desorption, which could ascribe to the variation of the local hardness of the activated carbon surfaces.

In this work, the HSAB principle, which was proposed by Pearson [22–24], and remains an important and widely used tool in chemistry today, would be used to explain the effects of the local hardness of the activated carbon surfaces on its adsorption of DBT. In this case, the HSAB principle was locally applied: "hard regions of a system prefer to interact with hard reagents whereas soft regions prefer soft species". To make a quantitative treatment of hardness, Parr and Pearson used the density functional theory (DFT). According to this, the absolute hardness and electronegativity of DBT can be estimated using following formula [23–25] from density functional theory (DFT) in order to confirm its soft/hard property.

$$\eta = \frac{1}{2}(I - A) \tag{2}$$

where η, the absolute hardness (always positive), is half the difference between I, the ionization energy, and A, the electron affinity. I and A can be found out by using the following equations:

$$I = -E_{HOMO} \tag{3}$$

$$A = -E_{LUMO} \tag{4}$$

Inserting Eqs. (3) and (4) into Eq. (2), one can get

$$\eta = -\frac{1}{2}(E_{HOMO} - E_{LUMO}) \tag{5}$$

and

$$\chi = \frac{1}{2}(I + A) = -\frac{1}{2}(E_{HOMO} + E_{LUMO}) \tag{6}$$

where E_{LUMO} is the lowest unoccupied molecular orbital (LUMO) orbital energy; E_{HOMO} the highest occupied molecular orbital (HOMO) orbital energy; χ is the electronegativity.

In this work, ab initio MO calculations for DBT were performed. The basis set was 3-21G, and Hyperchem 7.0 program systems were used to obtain the charge distribution, E_{LUMO} and E_{HOMO} of the DBT molecule. Then the hardness values and electronegativity of DBT were separately found out on the basis of Eqs. (2) and (6). The absolute hardness η of DBT was 5.267 and its electronegativity χ was 2.673. In terms of Pearson hard–soft base classification, DBT was considered as a soft base due to its absolute electronegativity $\chi < 2.8$ [22–24,26]. The computed results are listed in Table 2.

On the other hand, the transition metal ions were taken for Lewis acid [25]. According to Pearson classification, the ion Ag^+ belonged to soft, the ions Cu^{2+}, Ni^{2+}, and Zn^{2+} belonged to borderline acids, and the ion Fe^{3+} belonged to hard acid [25,29]. Table 3 shows the absolute hardness of these metal ions.

Table 2
E_{LUMO}, E_{HOMO}, hardness and electronegativity values for DBT (eV)

Molecule	DBT
E_{HOMO}	−7.939
E_{LUMO}	2.594
η	5.267
χ	2.673

Table 3
Pearson classification and absolute hardness of metal ions

Metal ions	Pearson classification	Absolute hardness, η
Ag^+	Soft	6.9
Cu^{2+}	Borderline	8.3
Ni^{2+}	Borderline	8.5
Zn^{2+}	Borderline	10.8
Fe^{3+}	Hard	13.1

When the different metal ions were separately loaded onto activated carbons by surface impregnation method, the surface local hardness of the activated carbon could be changed. The loading of soft acid ion Ag^+ led to the increase in the local soft acid of the activated carbon surfaces. According to a simple rule of the hard and soft acids and bases (HSAB) principle that hard acids prefer to bond to hard bases, and soft acids prefer to bond to soft bases [22–24,27–29], it can be predicted that the loading of Ag^+ would enhance the interaction between DBT and the Ag(I)/AC surfaces because Ag^+ was soft acid and DBT was soft base. In addition, it can be also predicted that the loading of Fe^{3+} would most possibly weaken the interaction between DBT and the Fe(III)/AC surfaces because Fe^{3+} was hard acid, while DBT was soft base. This prediction was agreement with the desorption activation energy of the DBT estimated from the TPD spectrums as shown in Table 1. That is to say, after the ion Ag^+ or Fe^{3+} was loaded onto the surfaces of the activated carbon, the activation energy of the DBT desorption on Ag(I)/AC became the highest, and that on Fe(III)/AC became the lowest. It should be noticed that the HSAB principle could not be used to predict what the interaction between the soft base and the borderline acids was. However, the results of the TPD experiments had indicated that the activation energy for the desorption of DBT on Zn(II)/AC, Ni(II)/AC and Cu(II)/AC was higher than that on the original activated carbon AC. The reasons may be that since the ions Zn^{2+}, Ni^{2+} and Cu^{2+} were borderline acids, the loading of ion Zn^{2+}, Ni^{2+} or Cu^{2+} on the surfaces of the activated carbon could weaken the local hard acids of the surfaces so that adsorption of DBT was enhanced to some extent.

From foregoing discussion, it can be seen that the use of the HSAB principle could interpret the effects of the metal ions being soft acid or hard acid separately loaded on the activated carbons on the activation energy of the DBT desorption.

5. Conclusions

The TPD spectrums of DBT on the activated carbons loaded separately with Ag^+, Cu^{2+}, Ni^{2+} and Zn^{2+} showed two distinct peaks, respectively corresponding to interaction of DBT with the activated carbon surface and with the metal ions on the other hand, which indicated producing new adsorption sites.

The activation energy for desorption of DBT on the various activated carbons follow the order: Ag(I)/AC > Zn(II)/AC > Ni(II)/AC > Cu(II)/AC > AC > Fe(III)/AC. In comparison with the original activated carbon, the loading of Ag^+ enhanced the interaction between DBT and the Ag(I)/AC surfaces because Ag^+ was soft acid and DBT was soft base, and the loading of Fe^{3+} weakened the interaction between DBT and the Fe(III)/AC surfaces because Fe^{3+} was hard acid, while DBT was soft base. The loading of the borderline acid ion Zn^{2+}, Ni^{2+} or Cu^{2+} on the surfaces of the activated carbon could weaken the local hard acids of the surfaces so that adsorption of DBT was enhanced to some extent.

Acknowledgment

The authors are very grateful to thank the National Natural Science Foundation of China (No. 20336020) for financial support.

References

[1] C. Song, An overview of new approaches to deep desulfurization for ultra-clean gasoline, diesel fuel and jet fuel, Catal. Today 86 (2003) 211–263.
[2] C. Song, X. Ma, New design approaches to ultra-clean diesel fuels by deep desulfurization and deep dearomatization, Appl. Catal. B: Environ. 41 (2003) 207–238.
[3] X. Ma, L. Sun, C. Song, A new approach to deep desulfurization of gasoline, diesel fuel and jet fuel by selective adsorption for ultra-clean fuels and for fuel cell applications, Catal. Today 77 (2002) 107–116.
[4] X. Ma, S. Velu, J.H. Kim, C. Song, Deep desulfurization of gasoline by selective adsorption over solid adsorbents and impact of analytical methods on ppm-level sulfur quantification for fuel cell applications, Appl. Catal. B: Environ. 56 (2005) 137–147.
[5] S. Velu, X. Ma, C. Song, Selective adsorption for removing sulfur from jet fuel over zeolite-based adsorbents, Ind. Eng. Chem. Res. 42 (2003) 5293–5304.
[6] C. Song, Fuel processing for low-temperature and high-temperature fuel cells: challenges and opportunities for sustainable development in the 21st century, Catal. Today 77 (2002) 17–49.
[7] S. Velu, X. Ma, C. Song, M. Namazian, S. Sethuraman, G. Venkataraman, Desulfuriation of JP-8 Jet fuel by selective adsorption over a Ni-based adsorbent for micro solid oxide fuel cells, Energy Fuels 19 (2005) 1116–1125.
[8] R.T. Yang, A.J. Hernandez-Maldonado, F.H. Yang, Desulfurization of transportation fuels with zeolites under ambient conditions, Science 301 (2003) 79–81.
[9] A.J. Hernandez-Maldonado, Yang S F.H., G.S. Qi, R.T. Yang, Desulfurization of transportation fuels by π-complexation sorbents: Cu(I)-, Ni(II)-, and Zn(II)-zeolites, Appl. Catal. B: Environ. 56 (2005) 111–126.
[10] A. Takahashi, F.H. Yang, R.T. Yang, New sorbents for desulfurization by π-complexation: thiophene/benzene adsorption, Ind. Eng. Chem. Res. 41 (2002) 2487–2496.
[11] A.J. Hernandez-Maldonado, S.D. Stamatis, R.T. Yang, A.Z. He, W. Cannella, New sorbents for desulfurization of diesel fuels via π-complexation: layered beds and regeneration, Ind. Eng. Chem. Res. 43 (2004) 769–776.
[12] S.H.A.B. Salem, Naphtha desulfurization by adsorption, Ind. Eng. Chem. Res. 33 (1994) 336–340.
[13] S.H.A.B. Salem, H.S. Hamid, Removal of sulfur compounds from naphtha solutions using solid adsorbents, Chem. Eng. Technol. 20 (1997) 342–347.
[14] J.H. Kim, X. Ma, A. Zhou, C. Song, Ultra-deep desulfurization and denitrogenation of diesel fuel by selective adsorption over three different adsorbents: a study on adsorptive selectivity and mechanism, Catal. Today 111 (2006) 74–83.
[15] A.J. Hernandez-Maldonado, R.T. Yang, Desulfurization of commercial liquid fuels by selective adsorption via π-complexation with Cu(I)–Y Zeolite, Ind. Eng. Chem. Res. 42 (2003) 3103–3110.

[16] H.X. Xi, Z. Li, H.B. Zhang, X. Li, X.J. Hu, Estimation of activation energy for desorption of low-volatility dioxins on zeolites by TPD technique, Sep. Purif. Technol. 31 (2003) 41–45.
[17] Z. Li, H.J. Wang, H.X. Xi, K.F. Xu, J. Wen, Estimation of activationenergy of desorption of *n*-hexane on activated carbons by TPD technique, Chin. J. React. Polym. 10 (2001) 113–120.
[18] I.M. Richard, Principles of Adsorption and Reaction on Solid Surfaces, First Edition, Wiley Series in Chemical Engineering, Wiley, New York, 1996, pp.482–580 (A Wiley-Interscience Publication).
[19] Q.B. Xia, Z. Li, H.X. Xi, K.F. Xu, Activation energy for dibenzofuran desorption from Fe^{3+}/TiO_2 and Ce^{3+}/TiO_2 photocatalysts coated onto glass fibers, Adsorpt. Sci. Technol. 23 (2005) 357–366.
[20] Z. Li, H.J. Wang, H.X. Xi, Q.B. Xia, J.L. Han, L.A. Luo, Estimation of activation energy of desorption of *n*-hexanol from activated carbons by the TPD technique, Adsorpt. Sci. Technol. 21 (2003) 125–133.
[21] Y.W. Wu, Z. Li, H.X. Xi, Influence of the microporosity and surface chemistry of polymeric resins on adsorptive properties toward phenol, J. Hazard. Mater. 113 (2004) 131–135.
[22] R.G. Pearson, Hard and soft acids and bases, J. Am. Chem. Soc. 85 (1963) 3533–3539.
[23] R.G. Parr, R.G. Pearson, Absolute hardness: companion parameter to absolute electronegativity, J. Am. Chem. Soc. 105 (1983) 7512–7516.
[24] R.G. Pearson, The HSAB principle—more quantitative aspects, Inorg. Chim. Acta 240 (1995) 93–98.
[25] A. Alfarraa, E. Frackowiakb, F. Beguin, The HSAB concept as a means to interpret the adsorption of metal ions onto activated carbons, Appl. Surf. Sci. 228 (2004) 84–92.
[26] J.X. Wang, Z.X. Liu, Y.L. Hu, Study on the new scale of hardness–softness for Lewis acid and bases, J. Northwest Normal Univ. (Nat. Sci.) 37 (2001) 95–99.
[27] R.C. Deka, K.R. Ram, Local reactivity descriptors to predict the strength of Lewis acid sites in alkali cation-exchanged zeolites, Chem. Phys. Lett. 389 (2004) 186–190.
[28] R.C. Deka, S. Pala, Influence of zeolite composition on the selectivity of alkylation reaction for the synthesis of *p*-isobutylethylbenzene: a computational study, Catal. Today 49 (1999) 221–227.
[29] M.V. Putz, N. Russo, E. Siclia, On the applicability of the HSAB principle through the use of improved computational schemes for chemical hardness evaluation, J. Comput. Chem. 25 (2004) 994–1003.